

Research



Cite this article: Zhang L, Evbuomwan OM, Tieu M, Zhao P, Martins AF, Sherry AD. 2017 Protonation of carboxyl groups in EuDOTA-tetraamide complexes results in catalytic prototropic exchange and quenching of the CEST signal. *Phil. Trans. R. Soc. A* **375**: 20170113.
<http://dx.doi.org/10.1098/rsta.2017.0113>

Accepted: 23 August 2017

One contribution of 10 to a discussion meeting issue 'Challenges for chemistry in molecular imaging'.

Subject Areas:

inorganic chemistry, biochemistry, chemical physics, organic chemistry, spectroscopy, physical chemistry

Keywords:

MRI contrast agent, Eu complex, pH sensor

Author for correspondence:

A. Dean Sherry

e-mail: dean.sherry@utsouthwestern.edu

Electronic supplementary material is available online at <https://dx.doi.org/10.6084/m9.figshare.c.3876118>.

Protonation of carboxyl groups in EuDOTA-tetraamide complexes results in catalytic prototropic exchange and quenching of the CEST signal

Lei Zhang¹, Osasere M. Evbuomwan³, Michael Tieu¹, Piyu Zhao¹, Andre F. Martins^{1,2} and A. Dean Sherry^{1,2}

¹Department of Chemistry and Biochemistry, University of Texas at Dallas, Richardson, TX 75080, USA

²Advanced Imaging Research Center, University of Texas Southwestern Medial Center, Dallas, TX, USA

³Department of chemistry and biochemistry, Gonzaga University, Spokane, WA 99258, USA

AFM, 0000-0002-0171-0261

The CEST properties of EuDOTA-tetraamide complexes bearing pendant carboxylate and carboxyl ethyl esters were measured as a function of pH. The CEST signal from the Eu³⁺-bound water molecule decreased in intensity between pH 8.5 and 4.5 while the proton exchange rates (k_{ex}) increased over this same pH range. In comparison, the CEST signal in the corresponding carboxyl ester derivatives was nearly constant. Both observations are consistent with stepwise protonation of the four carboxylic acid groups over this same pH range. This indicates that negative charges on the carboxyl groups above pH 6 facilitate the formation of a strong hydrogen-bonding network in the coordination second sphere above the single Eu³⁺-bound water molecule, thereby decreasing prototropic exchange of protons on the bound water molecule with bulk water protons. The percentage of square antiprismatic versus twisted square antiprism coordination isomers also decreased as the appended carboxylic acid groups were positioned further away from the amide. The net effect of lowering the pH was an overall increase in k_{ex} and a quenching of the CEST signal.

This article is part of the themed issue 'Challenges for chemistry in molecular imaging'.

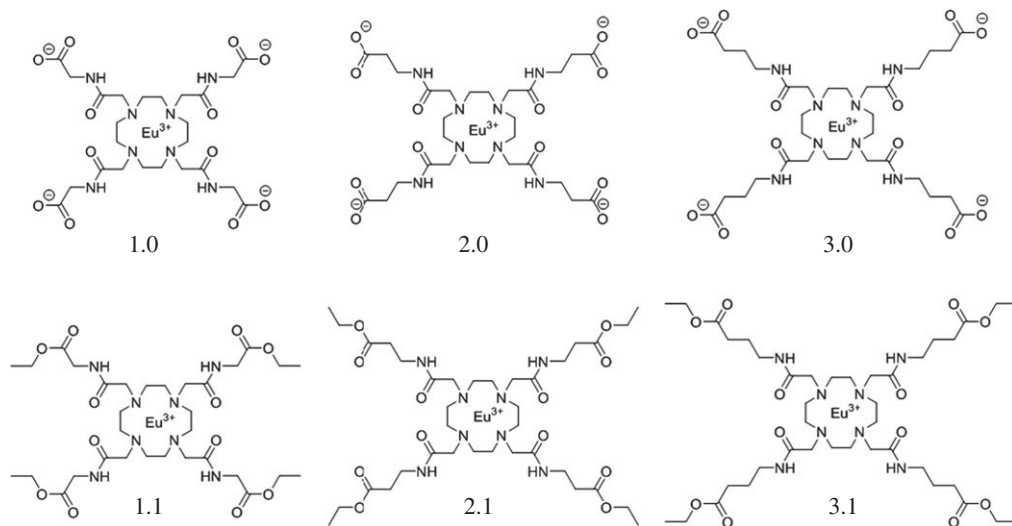
1. Introduction

The paramagnetic chemical exchange saturation transfer (paraCEST) agents present an attractive alternative to gadolinium-based agents for molecular imaging applications. Agents of this class typically consist of a lanthanide ion chelated by a macrocyclic derivative of DOTA and the contrast generated originates from the slow-to-intermediate exchange of the highly shifted lanthanide-bound water molecule with bulk water [1,2]. Given the ability of lanthanide ions to induce shifts in the resonances of proximate ligand protons, the exchange of highly shifted labile protons of amides and alcohols has also proved to be an efficient way of generating CEST contrast [3–5]. Eu^{3+} complexes of a variety of DOTA-tetraamide ligands have been most widely studied as water exchange-based paraCEST agents. The reasons for this popularity reside in the fact that water exchange is found to be slowest in Eu^{3+} complexes in comparison to other lanthanide complexes [6]. A second factor is that the weak electron donating properties of tetraamide oxygen donor atoms compared with DOTA itself results in a three- to fourfold decrease in the rate of water exchange between an inner-sphere Eu^{3+} -bound water molecule and bulk solvent, a condition highly favourable for CEST [7]. Furthermore, alteration of the DOTA-tetraamide structure has provided a way to design a variety of paraCEST agents responsive to physiological indicators such as pH [8,9], temperature [10,11], other metal ions [12–14], lactate [15,16] and enzyme activity [17,18]. Hence, the ability of these agents to provide functional information of this sort highlights their potential use as molecular imaging probes. The rate of proton exchange (k_{ex}) is one of the most important factors that determine CEST efficiency in these complexes [19], so most attempts to improve CEST sensitivity have been focused on designing paraCEST agents that exhibit slow proton exchange kinetics. The major factors influencing k_{ex} in Eu^{3+} -based agents are the coordination geometry of the complex and the nature of the ligand side chains. It was previously reported that introduction of carboxyl groups or carboxyl ethyl esters on the amide substituents of EuDOTA-tetraamide complexes would substantially decrease the bound water proton exchange rate. This observation has been explained by the hydrogen-bonding network between carboxyl groups and surrounding second-sphere water molecules that restrain proton exchange with the single inner-sphere water molecule. In this study, we sought to obtain a better understanding of the factors that influence the proton exchange rate in EuDOTA-tetraamide complexes. While a vast majority of studies of such complexes have focused on varying the functional groups on the amide side chains to alter the water molecule exchange rates, this study focused on how a change in pH alters the rate of exchange of protons between inner- and outer-sphere water molecules and how this impacts CEST sensitivity.

2. Results and discussion

Given that the EuDOTA-tetraamide complexes studied here (scheme 1) have fourfold symmetry, the relative proportions of SAP and TSAP coordination isomers can be estimated by integrating the area of a single, highly shifted ethylenediamine proton in the macrocyclic backbone (usually referred to as the H_4 proton). For Eu^{3+} complexes such as these, the H_4 proton resonance is typically found near 24–28 ppm in the SAP isomer and near 5–10 ppm in the TSAP isomer. The high-resolution ^1H NMR spectra of the three carboxylate complexes are shown in figure 1. It is evident that all three complexes exist mainly as SAP isomers. Closer examination of these ^1H NMR spectra reveals that a second H_4 resonance is also detectable in spectra of Eu-(2.0) and Eu-(3.0) near approximately 7 ppm, showing that a small amount of TSAP isomer is also present in the two complexes. The area of this resonance was found to increase as the length of the alkyl spacer between the amide group and the carboxyl group was increased.

Aime *et al.* [20] observed a similar trend with a few other Eu^{3+} complexes of DOTA-tetraamides wherein the SAP/TSAP ratio decreased in proportion to the number of alkyl groups on the amide. Thus, lengthening the alkyl spacer between the amide and carboxylic acid along the series, $\text{Eu}-(1.0) \rightarrow \text{Eu}-(2.0) \rightarrow \text{Eu}-(3.0)$, seems to favour the TSAP isomer. It is also interesting that in those complexes where the TSAP isomer can be observed, the H_4 proton resonances of



Scheme 1. Structures of the complexes used in this study.

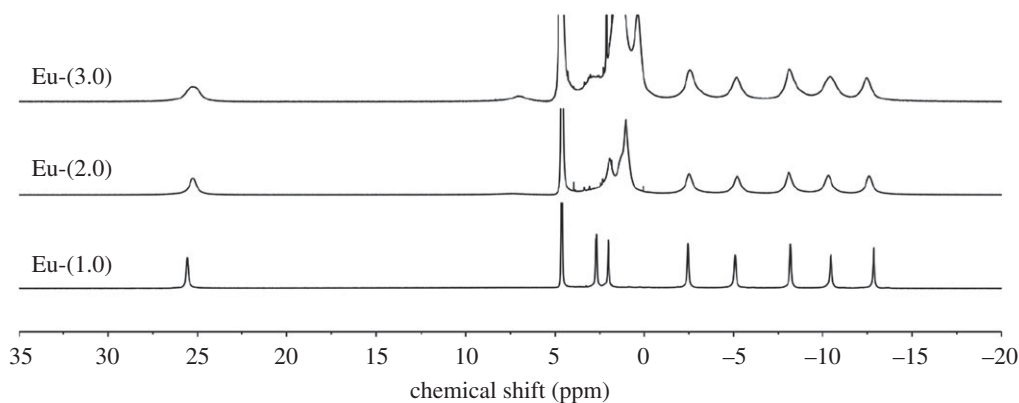


Figure 1. ^1H NMR spectra of three Eu^{3+} complexes recorded at 400 MHz in D_2O at pH 7.0.

both species are considerably broader. This indicates that the rate of interconversion between the SAP and TSAP isomers also increases as the length of the amide side chains was increased. This observation is useful in the design of paraCEST agents that preferentially exist as the SAP isomer in solution. The ^1H NMR spectra of the three carboxylate derivatives showed no change in the relative proportions of SAP and TSAP isomers over the pH range 4–9 (figure 2).

CEST spectra were also collected on these same three complexes as a function of pH. Several notable differences in these spectra were quite apparent (figure 3). First, the CEST intensity of the water molecule exchange peak near 50 ppm followed the same trend, $\text{Eu}-(1.0) \gg \text{Eu}-(2.0) > \text{Eu}-(3.0)$, at all pH values (see quantitative results in figure 3*d*). These differences were magnified under more acidic conditions. Since the CEST signal under observation here arises only from the SAP isomer present in solution (water exchange is too fast in the TSAP isomer), this partially reflects a decrease in population of the SAP isomer as the length of the alkyl group increases. The second notable difference relates to the pH dependency of the CEST intensities. Here, the intensity of the CEST signal of $\text{Eu}-(1.0)$ remains constant over the pH range 4–7 and slightly decreases above pH 8. In comparison, $\text{Eu}-(2.0)$ and $\text{Eu}-(3.0)$ display considerably different pH responses. Between pH 7.2 and approximately 6, the CEST is relatively constant but drops off

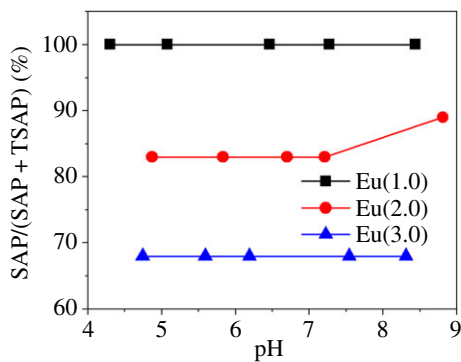


Figure 2. Plot of the proportion of SAP isomers as a function of pH.

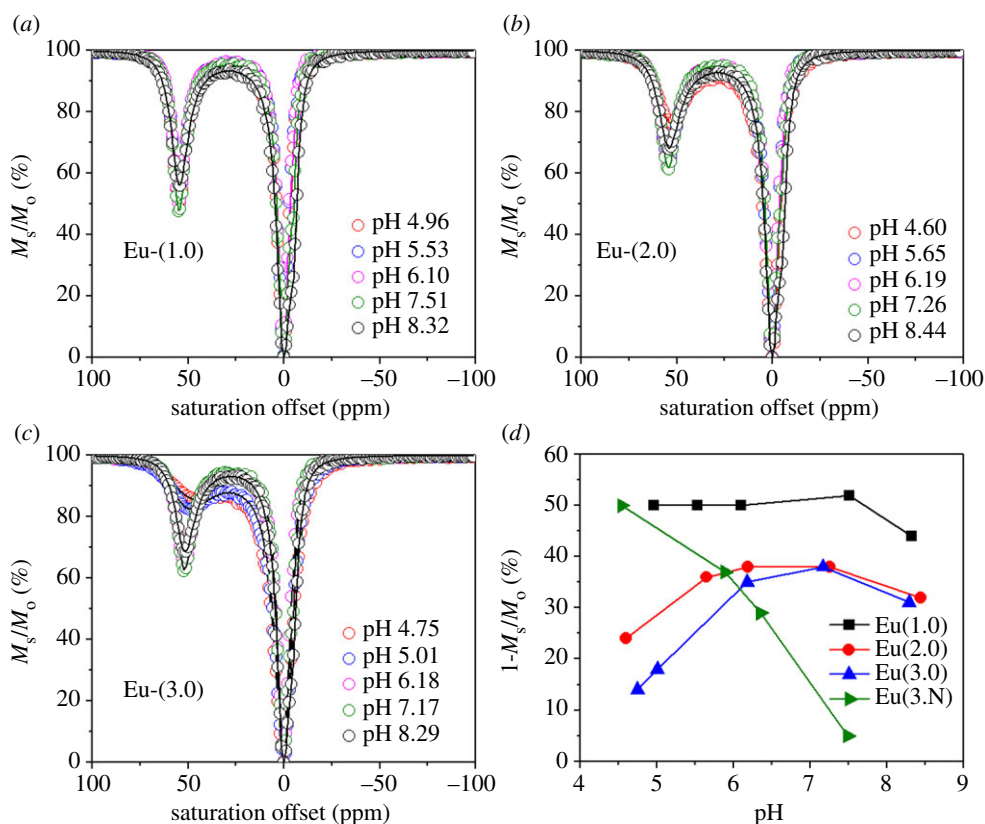


Figure 3. CEST spectra of 20 mM Eu complexes (a), (b) and (c) as a function of pH. A pre-saturation pulse of 600 Hz of 3 s was applied at 25°C. The solid lines reflect the fit of the experimental data to Bloch theory [21]. (d) CEST intensity as a function as pH.

at both high pH and low pH. At the lower pH values, the CEST signal of Eu-(3.0) decreases in intensity more than that of Eu-(2.0). These differences approximately parallel the estimated pK_a values of the extended carboxylate groups. The carboxylate groups in Eu-(1.0) would be expected to have pK_a 's similar to that of glycine, around 2–2.5, well below the range of pH values (4–7) examined here. The carboxylate groups in Eu-(2.0) should be similar to the pK_a of the γ carboxyl group in aspartic acid, around 4.5. Consequently, the decrease in CEST intensity below pH approximately 5.5 is consistent with the initial stages of protonation of the carboxyl groups

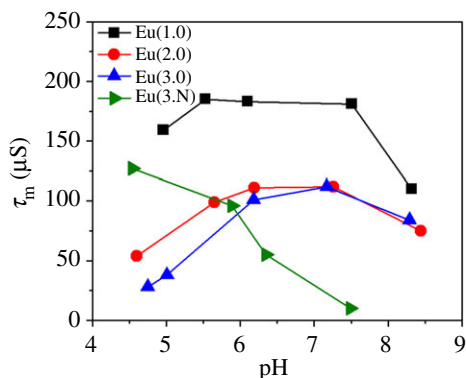


Figure 4. Plot of bound water proton residence lifetime (τ_m) as a function of pH at 25°C.

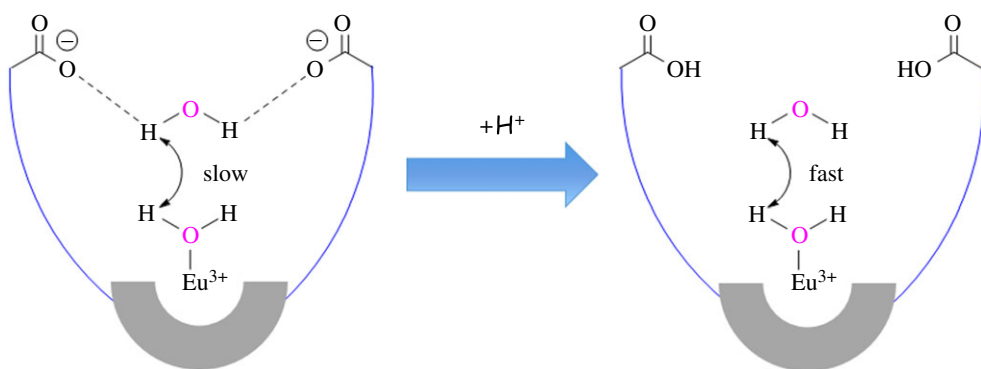


Figure 5. Schematic of the prototropic effects described in this study. (Left) An ionized carboxyl group (COO^-) forms a strong hydrogen-bonding network that slows prototropic exchange of all water protons. (Right) Protonated carboxyl groups form a weak hydrogen-bonding network thereby allowing rapid proton exchange between bulk water protons and the protons on the Eu^{3+} -bound water molecule.

in this complex. Among these three complexes, the carboxyl groups in Eu-(3.0) are predicted to have the highest pK_a values, consistent with a greater decrease in CEST signal that begins above pH 6 and drops more rapidly as the pH is lowered even further. The green line and data points in figure 3d show similar pH-dependent CEST data for a EuDOTA-tetraamide complex having three appended primary amine groups (labelled Eu-(3.N), an amine analogue of Eu-(3.0). More details of the amine series will be published elsewhere. However, it is interesting to note that in the case of the amine derivative, the pH dependence of CEST is opposite to those complexes described here. In Eu-(3.N), the CEST signal is small at pH 7.4, but increases as almost linearly to pH 4.5 as the amines become protonated. Hence, protonation of appended carboxyl groups results in quenching of the CEST signal while protonation of appended amine groups results in significant enhancement of the CEST signal.

What is the origin of these interesting differences? As indicated in the introduction, the CEST intensity is highly dependent upon proton exchange rates in all complexes. To verify that these CEST changes are related to differences in proton exchange rates, each of the CEST spectra were fitted to Bloch theory for a two-site exchange model [21]. The resulting values are shown in figure 4. Not surprisingly, the trends shown in figure 4 for proton exchange rates largely parallel the CEST effects illustrated in figure 3d. The proton lifetimes ($\tau_m = 1/k_{\text{ex}}$) show that protonation

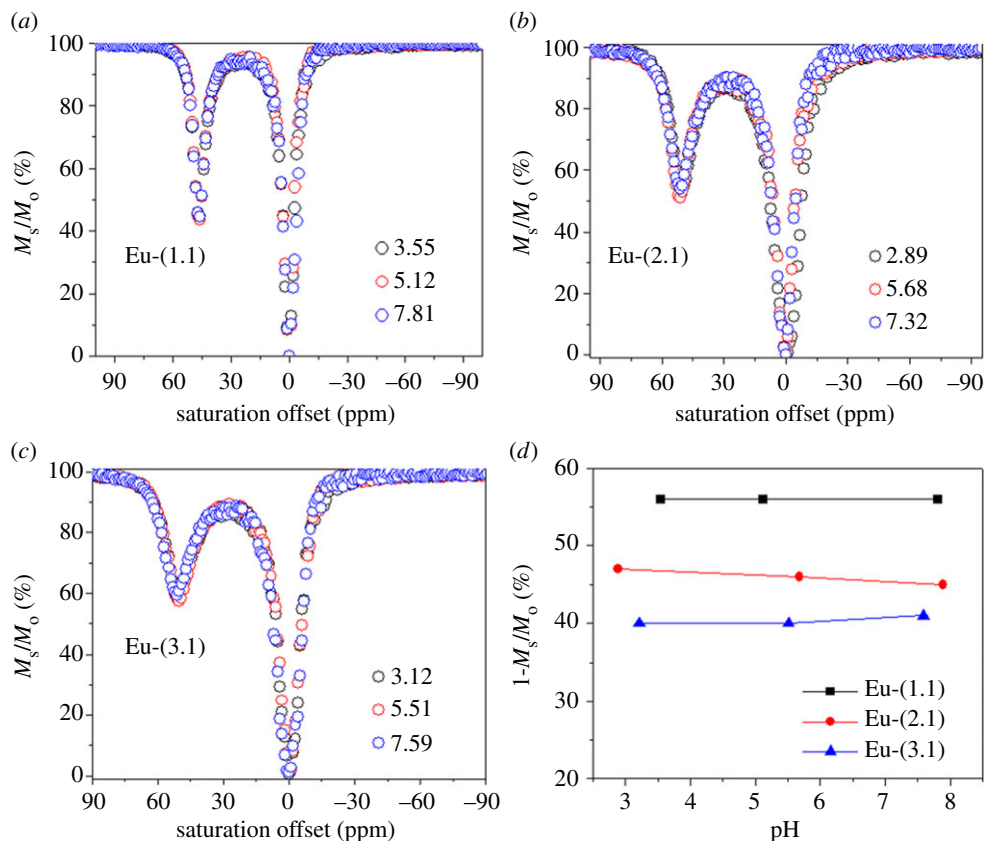


Figure 6. CEST spectra of 20 mM Eu complexes (a), (b) and (c) as a function of pH. A pre-saturation pulse of 600 Hz of 3 s was applied at 25°C. (d) CEST intensity as a function as pH.

of a carboxyl group results in faster proton exchange and a parallel decrease in CEST intensity. This indicates that negatively charged carboxyl groups located near the Eu^{3+} -bound water results in a decreased prototropic exchange of bulk water protons with the bound water protons. A carboxylate anion is more electron donating and can participate in more extensive hydrogen-bonding (H-bonding) networks with water molecules in the second coordination sphere. This hydrogen-bonding network serves to stabilize the Eu^{3+} -bound water molecule, slowing-down or impeding proton exchange with bulk water and thereby enhancing the CEST intensity (figure 5) [22–26]. Above pH 8, a second factor, base-catalysed proton exchange, begins to play a role in the exchange kinetics and hence the CEST signal once again becomes quenched.

In additional support of these conclusions, we also prepared the corresponding ethyl ester derivatives of these same complexes. As shown in figure 6, the CEST signal of these complexes is not sensitive to changes in pH between 3 and 7.5. In this case, the ester-protected carboxyl groups cannot accept protons so remain pH insensitive over this entire pH range. At higher pH, these systems also show a decrease in pH due to base-catalysed exchange of protons.

3. Conclusions

In this study, the CEST properties of a series of EuDOTA-tetraamides bearing carboxylic acid, ester or amine substituents were studied as a function of pH. The results indicate that lengthening the alkyl spacer between the amide and the carboxylic acid functional group results in an increase in the population of TSAP isomer that parallels the increasing bulkiness of the amide pendant

arms. It was shown that the pH dependence of CEST in these complexes is governed by the rate prototropic exchange between bulk solvent water protons and Eu^{3+} -bound water protons. Protonation of appended carboxyl groups results in an increase in the rate of prototropic exchange and subsequent quenching of the CEST signal. The most favourable ionic forms for agents of this type are negatively charged carboxyl groups positioned above the central Eu^{3+} -bound water molecule. The resulting hydrogen-bonding network stabilizes all protons in the immediate vicinity of the Eu-bound water molecule and this helps to maximize the CEST effect. The opposite is observed for complexes containing appended amine groups. In those complexes, protonation of the amine groups serves to stabilize the hydrogen-bonding network and increase CEST. Thus, any functional group that stabilizes protons in an inner-/outer-sphere network is advantageous for CEST enhancement. This work demonstrates that the development of paraCEST agents that are responsive to important biomarkers such as the pH can be optimized and tuned so that they can be used in a variety of possible medical applications. Finally, it is worth considering the potential applicability of this method for imaging pH in tumours, acidosis and kidney failure. Although the paraCEST agents mentioned in this work might still be limited by the inherent low sensitivity of the technique, this limitation can be easily overcome by delivering these agents in the form of nanoparticles or macromolecules (liposomes, dendrimers, polymers, viruses, lipoproteins, etc.). The delivery of these particles into the extracellular space can increase the sensitivity of the paraCEST agents by several orders of magnitude by accumulation and/or by simple tissue perfusion.

Data accessibility. All relevant data can be found in this paper and the electronic supplementary material.

Authors' contributions. L.Z., O.M.E. and A.D.S. carried out the experiments. L.Z., O.M.E., A.F.M. and P.Z. performed the data analysis. O.M.E., L.Z., A.F.M. and A.D.S. drafted the manuscript. All authors read and approved the manuscript'.

Competing interests. We declare we have no competing interest.

Funding. The authors acknowledge partial financial support for this work from the National Institutes of Health (CA-115531, EB-01598), Harold C. Simmons Cancer Center through an NCI Cancer Center Support Grant, 1P30 CA142543, and the Robert A. Welch Foundation (AT-584).

References

1. Zhang S, Wu K, Biewer MC, Sherry AD. 2001 ^1H and ^{17}O NMR detection of a lanthanide-bound water molecule at ambient temperatures in pure water as solvent. *Inorg. Chem.* **40**, 4284–4290. (doi:10.1021/ic0003877)
2. Zhang S, Winter P, Wu K, Sherry AD. 2001 A novel europium(III)-based MRI contrast agent. *J. Am. Chem. Soc.* **123**, 1517–1518. (doi:10.1021/ja005820q)
3. Woods M, Woessner DE, Zhao P, Pasha A, Yang M-Y, Huang C-H, Vasalitiy O, Morrow JR, Sherry AD. 2006 Europium(III) macrocyclic complexes with alcohol pendant groups as chemical exchange saturation transfer agents. *J. Am. Chem. Soc.* **128**, 10155–10162. (doi:10.1021/ja061498t)
4. Aime S, Delli Castelli D, Terreno E. 2002 Novel pH-reporter MRI contrast agents. *Angew. Chem. Int. Ed.* **41**, 4334–4336. (doi:10.1002/1521-3773(20021115)41:22<4334::AID-ANIE4334>3.0.CO;2-1)
5. Zhang S, Michaudet L, Burgess S, Sherry AD. 2002 The Amide protons of an ytterbium(III) dota tetraamide complex act as efficient antennae for transfer of magnetization to bulk water. *Angew. Chem. Int. Ed.* **41**, 1919–1921. (doi:10.1002/1521-3773(20020603)41:11<1919::AID-ANIE1919>3.0.CO;2-Q)
6. Zhang S, Wu K, Sherry AD. 2002 Unusually sharp dependence of water exchange rate versus lanthanide ionic radii for a series of tetraamide complexes. *J. Am. Chem. Soc.* **124**, 4226–4227. (doi:10.1021/ja017133k)
7. Viswanathan S, Kovacs Z, Green KN, Ratnakar SJ, Sherry AD. 2010 Alternatives to gadolinium-based metal chelates for magnetic resonance imaging. *Chem. Rev.* **110**, 2960–3018. (doi:10.1021/cr900284a)
8. Aime S, Barge A, Delli Castelli D, Fedeli F, Mortillaro A, Nielsen FU, Terreno E. 2002 Paramagnetic Lanthanide(III) complexes as pH-sensitive chemical exchange saturation

- transfer (CEST) contrast agents for MRI applications. *Magn. Reson. Med.* **47**, 639–648. (doi:10.1002/mrm.10106)
9. Wu Y, Zhou Y, Ouari O, Woods M, Zhao P, Soesbe TC, Kiefer GE, Sherry AD. 2008 Polymeric PARACEST Agents for Enhancing MRI Contrast Sensitivity. *J. Am. Chem. Soc.* **130**, 13 854–13 855. (doi:10.1021/ja805775u)
 10. Li AX, Wojciechowski F, Suchy M, Jones CK, Hudson RHE, Menon RS, Bartha R. 2008 A sensitive PARACEST contrast agent for temperature MRI: Eu³⁺-DOTAM-glycine (Gly)-phenylalanine (Phe). *Magn. Reson. Med.* **59**, 374–381. (doi:10.1002/mrm.21482)
 11. Zhang S, Malloy CR, Sherry AD. 2005 MRI Thermometry Based on PARACEST Agents. *J. Am. Chem. Soc.* **127**, 17 572–17 573. (doi:10.1021/ja053799t)
 12. Esqueda AC, López JA, Andreu-de-Riquer G, Alvarado-Monzón JC, Ratnakar J, Lubag AJM, Sherry AD, De León-Rodríguez LM. 2009 A new gadolinium-based MRI Zinc sensor. *J. Am. Chem. Soc.* **131**, 11 387–11 391. (doi:10.1021/ja901875v)
 13. Cotruvo Jr JA, Aron AT, Ramos-Torres KM, Chang CJ. 2015 Synthetic fluorescent probes for studying copper in biological systems. *Chem. Soc. Rev.* **44**, 4400–4414. (doi:10.1039/C4CS00346B)
 14. Ramos-Torres KM, Kolemen S, Chang CJ. 2016 Thioether coordination chemistry for molecular imaging of copper in biological systems. *Isr. J. Chem.* **56**, 724–737. (doi:10.1002/ijch.201600023)
 15. Zhang L *et al.* 2017 Imaging extracellular lactate *in vitro* and *in vivo* using CEST MRI and a paramagnetic shift reagent. *Chem - Eur J.* **23**, 1752–1756. (doi:10.1002/chem.201604558)
 16. Aime S, Delli Castelli D, Fedeli F, Terreno E. 2002 A Paramagnetic MRI-CEST agent responsive to lactate concentration. *J. Am. Chem. Soc.* **124**, 9364–9365. (doi:10.1021/ja0264044)
 17. Yoo B, Pagel MD. 2006 A PARACEST MRI contrast agent to detect enzyme activity. *J. Am. Chem. Soc.* **128**, 14 032–14 033. (doi:10.1021/ja063874f)
 18. Chauvin T, Durand P, Bernier M, Meudal H, Doan B-T, Noury F, Badet B, Beloeil J-C, Tóth E. 2008 Detection of enzymatic activity by PARACEST MRI: a general approach to target a large variety of enzymes. *Angew. Chem. Int. Ed.* **47**, 4370–4372. (doi:10.1002/anie.200800809)
 19. Sherry AD, Wu Y. 2013 The importance of water exchange rates in the design of responsive agents for MRI. *Curr. Opin. Chem. Biol.* **17**, 167–174. (doi:10.1016/j.cbpa.2012.12.012)
 20. Aime S, Barge A, Bruce JI, Botta M, Howard JAK, Moloney JM, Parker D, de Sousa AS, Woods M. 1999 NMR, relaxometric, and structural studies of the hydration and exchange dynamics of cationic lanthanide complexes of macrocyclic tetraamide ligands. *J. Am. Chem. Soc.* **121**, 5762–5771. (doi:10.1021/ja990225d)
 21. Woessner DE, Zhang S, Merritt ME, Sherry AD. 2005 Numerical solution of the bloch equations provides insights into the optimum design of PARACEST agents for MRI. *Magn. Reson. Med.* **53**, 790–799. (doi:10.1002/mrm.20408)
 22. Liepinsh E, Otting G. 1996 Proton exchange rates from amino acid side chains—implications for image contrast. *Magn. Reson. Med.* **35**, 30–42. (doi:10.1002/mrm.1910350106)
 23. Aime S, Botta M, Fasano M, Terreno E. 1999 Prototropic and water-exchange processes in aqueous solutions of Gd(III) chelates. *Acc. Chem. Res.* **32**, 941–949. (doi:10.1021/ar970300u)
 24. Kálmán FK, Woods M, Caravan P, Jurek P, Spiller M, Tircsó G, Király R, Brücher E, Sherry AD. 2007 Potentiometric and relaxometric properties of a gadolinium-based MRI contrast agent for sensing tissue pH. *Inorg. Chem.* **46**, 5260–5270. (doi:10.1021/ic0702926)
 25. Woods M, Pasha A, Zhao P, Tircso G, Chowdhury S, Kiefer G, Woessner DE, Sherry AD. 2011 Investigations into whole water, prototropic and amide proton exchange in lanthanide(iii) DOTA-tetraamide chelates. *Dalton Trans.* **40**, 6759–6764. (doi:10.1039/c1dt10616c)
 26. Delli Castelli D, Terreno E, Aime S. 2011 YbIII-HPDO3A: a dual ph- and temperature-responsive CEST agent. *Angew. Chem. Int. Ed.* **50**, 1798–1800. (doi:10.1002/anie.201007105)